chemosensors

Supplementary Materials for

"Out of pocket "Protein Binding—A Dilemma of Epitope Imprinted Polymers Revealed for Human Hemoglobin

Xiaorong Zhang [1,†], Giorgio Caserta [2,†], Aysu Yarman [1], Eszter Supala [3], Armel F. Tadjoung Waffo [2], Ulla Wollenberger [1], Róbert E. Gyurcsányi [3,*], Ingo Zebger [2,*] and Frieder W. Scheller [1,*]

(A)

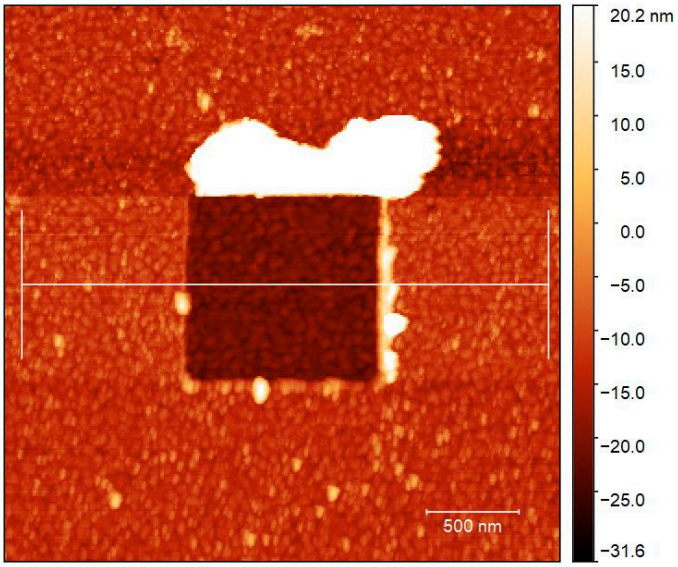

(B)

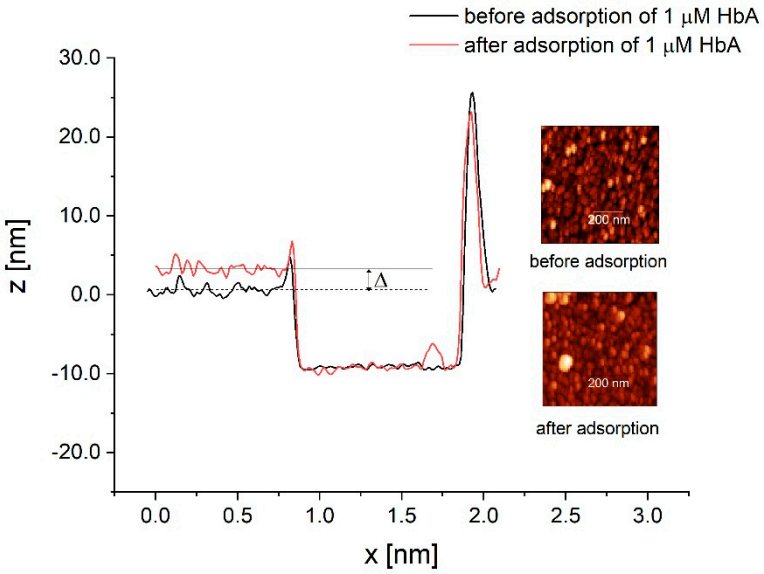

Figure S1. (**A**) The topographic images of the non-imprinted polymer film were used for the thickness measurements after removal of a 1 × 1 μm rectangular area from the polymer. The removal stops at the underlying gold surface. The bright regions are due to removed material pushed to the sides of the rectangular area during the removal process. The difference of the film

thickness (Δ) after and before adsorption of 1μM HbA, as illustrated in the representative cross-sectional profiles (**B**), indicates the adsorption of HbA (see Table 2 for quantitative data).

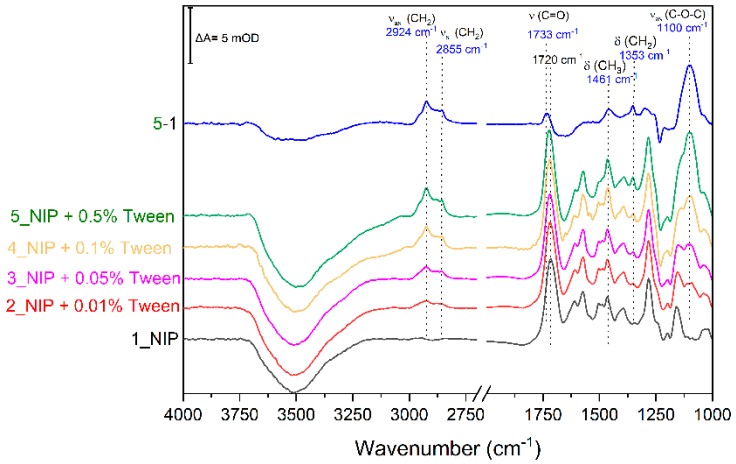

Figure S2. IR absorbance spectra of Tween binding on polyscopoletin (NIP). Spectra were recorded using different concentrations of Tween (0.01 % - trace 2, red; 0.05 % - trace 3, magenta; 0.1 % - trace 4, yellow; 0.5 % - trace 5, green) and compared to the bare NIP shown in dark trace 1. The binding of Tween (0.05 %) is better visualized in the corresponding difference spectrum between trace 5 and trace 1. Here, the observed bands are attributed to the ν(C-O-C) stretching vibration mode of -CH_2-O-CH_2- chains (1100 cm^{-1}), the δ(CH_2) bending mode from the ethylene subunit (1451 cm^{-1} and 1353 cm^{-1}), the ν(C=O) stretching mode arising from the carbonyl groups (1733 cm^{-1}), and the asymmetric and symmetric methylene stretching vibration modes ν(CH_2) at 2924 cm^{-1} and 2855 cm^{-1}, respectively [1].

Table S1. MIPs prepared by epitope approaches.

Peptide-MIPs						
Template	**MIP structure**	**Epitope/peptide**	**Selectivity**	**Linear measuring range**	**IF and K_d**	**Reference**
HbA	Free radical polymerization of peptides-decorated silica beads followed by removal of silica	N-terminal sequences of both α- and β-chain	BSA, Mb	n.d.	IF = ~ 1.7 for HbA	[2]
Insulin	EP of *o*-PD on epitope modified gold surface	C-terminal peptide	Insulin in serum samples	10 - 500 fM for insulin	n.d.	[3]
Cyt c, ADH, BSA	Photopolymerization of MIP on a glass or silicon surface	C-terminal nonapeptides of each protein	Exchange of one amino acid	0 - 289 nM for Cyt c	K_d = 72.3 nM IF = 7 for Cyt c	[4]
Cyt c	EP of scopoletin on gold	Cys-extended C-terminal nonapeptide	BSA, Mb	0 - 10 μM for Cyt c	K_d = 8.54 μM and 2.51 μM, IF = 6 and 10 for Cyt c and epitope	[5]
Cyt c	Thermo-sensitive CDs/SiO_2/MIP	C- and N-terminal nonapeptides	Lysozyme, trypsin	0.1- 40 μM for Cyt c	IF = 5.65 for Cyt c	[6]
Trf	Epitope imprinted PES beads	N-terminal peptide	RNase B, Cyt c, β-LG	n.d.	n.d.	[7]
HSA, IgG, Trf	Multiepitope imprinted PES particles	N-terminal peptides of each protein	Proteins in human plasma	n.d.	n.d.	[8]
HSA, Trf	Dual-template imprinted polymer on MCNTs	C-terminal peptides of each protein	BSA, Mb, Cyt C	n.d.	IF = 2.57 for HSA IF = 2.17 for Trf	[9]
NSE	EP of scopoletin on the peptide modified QCM chips	NSE derived synthetic peptide	Nonspecific peptides and BSA	n.d.	K_d = 12.2 μM and 53 pM for peptide and NSE IF = 4.6 for NSE	[10]
IgG	Polymerization of the template modified glass beads	Fc domain	n.d.	n.d.	K_d = 27.4 nM for IgG	[11]
Cyt c	Reverse microemulsion polymerization of APTES on QCM	C-terminus octapeptide	Mb, HSA, HRP, human serum	0.40 – 4.0 nM for Cyt c	IF = 3.0 for Cyt c	[12]
B2M	Polycondensation of multiple silylating reagents	C-terminus nonapeptide	RNase A, RNase B, HRP, BSA	n.d.	K_d = 0.2 μM and IF = 5.8 for epitope IF = 5.0 for B2M	[13]
Apha-synuclein	EP of AN/MSAN with various peptides on screen-printed	3 peptides encompassed locations of mutations	Real sample: Culture medium from the	n.d.	n.d.	[14]

	electrodes	differentiation of midbrain organoids				
			Tag-MIPs			
HSA	Self-polymerization of dopamine on Ni^{2+} modified magnetic NPs	His-tag-anchored C-terminal peptide	BSA, Cyt c	n.d.	IF = 4.26 for epitope IF = 2.12 for HSA	[15]
HSA	Thermosensitive MIP on modified SiO_2 NPs	His-tag-anchored C-terminal peptide	BSA, Mb, RNase B	9 - 15 μM for HSA	IF = 4.0 for HSA	[16]
GFP	His_6-tag imprinted on the IMAC matrix surface	His-tag (HHHHHH)	GFP from the crude cell lysis	n.d.	IF = 7.1 for GFP	[17]
CD56	EP of *p*-ABA and template	Poly-sialic acid	CA19-9, PSA, BSA, BHb	0.07 – 1.07 pM for CD56	n.d.	[18]
CA 19-9	EP of *o*-PD and template on a GCE	Monosaccharide or polysaccharide	BHb, BSA, Con A	1 - 60 U/mL and 0.1 – 5 U/mL for monosaccharide and polysaccharide imprinted MIP	n.d.	[19]

Abbreviations: ADH: Alcohol dehydrogenase; AN: Aniline; APTES: Amino-propyltriethoxysilane; BHb: Bovine hemoglobin; B2M: β2-Microglobulin; *β*-LG: *β*-Lactoglobulin; BSA: Bovine serum albumin; CA19-9: Carbohydrate antigen 19-9; CD56: A neural cell adhesion molecule; CDs: Carbon dots; ConA: Concanavalin A; Cyt c: Cytochrome c; EP: Electropolymerization; GCE: Glassy carbon electrode; GFP: Green fluorescent protein; HSA: Human serum albumin; HRP: Peroxidase horseradish; IgG: Immunoglobulin G; IMAC: Immobilized metal ion affinity chromatography; *o*-PD: *o*-Phenylenediamine; *p*-ABA: *p*-Aminobenzeneboronic acid; PES: Poly(ether sulfone); PSA: Prostate-specific antigen; Mb: Myoglobin; MCNTs: Magnetic carbon nanotubes; MSAN: *m*-Aminobenzenesulfonic acid; n.d.: Not determined; NPs: Nanoparticles; NSE: Neuron specific enolase; QCM: Quartz crystal microbalance sensor; RNase B: Ribonuclease B.

References

1. Warring, S.L.; Krasowska, M.; Beattie, D.A.; McQuillan, A.J. Adsorption of a Polyethoxylated Surfactant from Aqueous Solution to Silica Nanoparticle Films Studied with in Situ Attenuated Total Reflection Infrared Spectroscopy and Colloid Probe Atomic Force Microscopy. *Langmuir* **2018**, *34*, 13481–13490.
2. Bagán, H.; Zhou, T.; Eriksson, N.L.; Bülow, L.; Ye, L. Synthesis and characterization of epitope-imprinted polymers for purification of human hemoglobin. *RSC Adv.* **2017**, *7*, 41705–41712.
3. Zhao, C.; Ma, X.; Li, J. An Insulin Molecularly Imprinted Electrochemical Sensor Based on Epitope Imprinting. *Chinese J. Anal. Chem.* **2017**, *45*, 1360–1366.
4. Nishino, H.; Huang, C.-S.; Shea, K.J. Selective Protein Capture by Epitope Imprinting. *Angew. Chemie Int. Ed.* **2006**, *45*, 2392–2396.
5. Dechtrirat, D.; Jetzschmann, K.J.; Stöcklein, W.F.M.; Scheller, F.W.; Gajovic-Eichelmann, N. Protein Rebinding to a Surface-Confined Imprint. *Adv. Funct. Mater.* **2012**, *22*, 5231–5237.
6. Li, D.-Y.; Zhang, X.-M.; Yan, Y.-J.; He, X.-W.; Li, W.-Y.; Zhang, Y.-K. Thermo-sensitive imprinted polymer embedded carbon dots using epitope approach. *Biosens. Bioelectron.* **2016**, *79*, 187–192.
7. Yang, K.; Liu, J.; Li, S.; Li, Q.; Wu, Q.; Zhou, Y.; Zhao, Q.; Deng, N.; Liang, Z.; Zhang, L.; et al. Epitope imprinted polyethersulfone beads by self-assembly for target protein capture from the plasma proteome. *Chem. Commun.* **2014**, *50*, 9521–9524.
8. Yang, K.; Li, S.; Liu, J.; Liu, L.; Zhang, L.; Zhang, Y. Multiepitope Templates Imprinted Particles for the Simultaneous Capture of Various Target Proteins. *Anal. Chem.* **2016**, *88*, 5621–5625.
9. Qin, Y.-P.; Jia, C.; He, X.-W.; Li, W.-Y.; Zhang, Y.-K. Thermosensitive Metal Chelation Dual-Template Epitope Imprinting Polymer Using Distillation–Precipitation Polymerization for Simultaneous Recognition of Human Serum Albumin and Transferrin. *ACS Appl. Mater. Interfaces* **2018**, *10*, 9060–9068.
10. Altintas, Z.; Takiden, A.; Utesch, T.; Mroginski, M.A.; Schmid, B.; Scheller, F.W.; Süssmuth, R.D. Integrated Approaches Toward High-Affinity Artificial Protein Binders Obtained via Computationally Simulated Epitopes for Protein Recognition. *Adv. Funct. Mater.* **2019**, *29*, 1807332.
11. Moczko, E.; Guerreiro, A.; Cáceres, C.; Piletska, E.; Sellergren, B.; Piletsky, S.A. Epitope approach in molecular imprinting of antibodies. *J. Chromatogr. B Anal. Technol. Biomed. Life Sci.* **2019**, *1124*, 1–6.
12. Ma, X.T.; He, X.W.; Li, W.Y.; Zhang, Y.K. Oriented surface epitope imprinted polymer-based quartz crystal microbalance sensor for cytochrome c. *Talanta* **2019**, *191*, 222–228.
13. Xing, R.; Ma, Y.; Wang, Y.; Wen, Y.; Liu, Z. Specific recognition of proteins and peptides via controllable oriented surface imprinting of boronate affinity-anchored epitopes. *Chem. Sci.* **2019**, *10*, 1831–1835.
14. Lee, M.H.; Thomas, J.L.; Su, Z.L.; Yeh, W.K.; Monzel, A.S.; Bolognin, S.; Schwamborn, J.C.; Yang, C.H.; Lin, H.Y. Epitope imprinting of alpha-synuclein for sensing in Parkinson's brain organoid culture medium. *Biosens. Bioelectron.* **2021**, *175*, 112852.
15. Li, S.; Yang, K.; Liu, J.; Jiang, B.; Zhang, L.; Zhang, Y. Surface-Imprinted Nanoparticles Prepared with a His-Tag-Anchored Epitope as the Template. *Anal. Chem.* **2015**, *87*, 4617–4620.
16. Li, S.; Yang, K.; Deng, N.; Min, Y.; Liu, L.; Zhang, L.; Zhang, Y. Thermoresponsive Epitope Surface-Imprinted Nanoparticles for Specific Capture and Release of Target Protein from Human Plasma. *ACS Appl. Mater. Interfaces* **2016**, *8*, 5747–5751.
17. Li, S.; Yang, K.; Zhao, B.; Li, X.; Liu, L.; Chen, Y.; Zhang, L.; Zhang, Y. Epitope imprinting enhanced IMAC (EI-IMAC) for highly selective purification of His-tagged protein. *J. Mater. Chem. B* **2016**, *4*, 1960–1967.

18. Ma, X.; Li, M.; Tong, P.; Zhao, C.; Li, J.; Xu, G. A strategy for construction of highly sensitive glycosyl imprinted electrochemical sensor based on sandwich-like multiple signal enhancement and determination of neural cell adhesion molecule. *Biosens. Bioelectron.* **2020**, *156*, 112150.
19. Li, J.; Ma, X.; Li, M.; Zhang, Y. Does polysaccharide is an idea template selection for glycosyl imprinting? *Biosens. Bioelectron.* **2018**, *99*, 438–442.